

Surface-Condition Detection System of Drone-Landing Space using Ultrasonic Waves and Deep Learning

Masatoshi Hamanaka, and Fujio Nakano

Abstract— We propose a system for detecting the surface conditions of a landing space using ultrasonic sensors mounted on a drone. The advantage of ultrasonic sensors is that they are extremely low cost, are much lighter and smaller than cameras, have millimeter-wave lasers, and use LiDAR. However, normal ultrasonic sensors can only measure the distance from the nearest object, so the amount of information is insufficient to estimate the conditions of a landing space. Therefore, we propose installing an ultrasonic sensor on each arm of the drone and estimating the condition of the landing space from the time series of reflected waves for very short ultrasonic waves. In the measurement results, reflected waves were small and changed irregularly for each sensor where a space was not suitable for landing. In a simulation experiment using deep learning, our system was able to determine whether a condition was suitable for landing with an accuracy of 98%.

I. INTRODUCTION

We propose a system for small lightweight drones to land safely at unknown locations. Some drones have a ‘go home’ feature that automatically returns them to their take-off positions if they lose communication with the base station or receive a return signal. However, drones often crash due to running out of battery while returning. Additionally, when returning, they return in a straight line instead of the route they flew, so if there is an obstacle along the return flight path, they will crash into it (Fig. 1). In some cases, the risk of a crash can be reduced by having the drone land as soon as possible rather than return to the take-off position.

Small lightweight drones are easily unbalanced by the wind and can crash when landing. For example, in an area of thick vegetation, leaves can easily wind around a propeller just before the drone lands. In addition, if the landing space is rocky, the drone may come into contact with the rocks during landing and lose balance.

Systems using a QR code or marker have been proposed for landing drones safely [1–3]. However, such systems assume a flat landing space. Therefore, if the drone is swept away by the wind or an abnormal event occurs that necessitates an emergency landing, the drone needs to evaluate the surface conditions of the landing space.

Systems for preventing collisions have been proposed, including those using Visual Simultaneous Localization and Mapping (SLAM) [4, 5], range-finding sensors [6], light detection and ranging (LiDAR) [7, 8], and stereo cameras [9, 10]. Although these systems are mainly used for detecting obstacles in the direction of drone movement, they may be able to evaluate the surface conditions of the landing space by

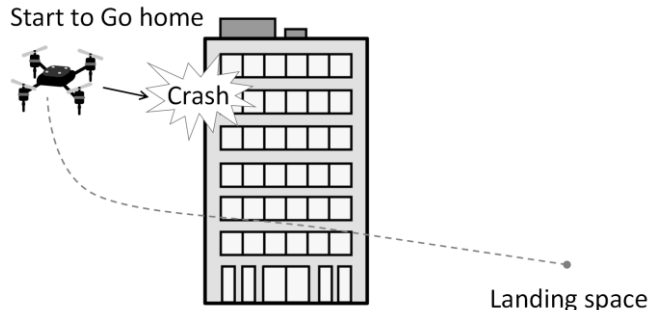


Figure 1. Example of drone crashing while returning home

determining the sensor-installation direction. In a system that estimates the position from the ground surface shape, however, the LiDAR sensor is mounted pointing downward, enabling it to sense the landing space [11]. However, LiDAR adds a large payload to these systems, so they are difficult to apply to small lightweight drones.

A lightweight automatic landing system has been achieved by image processing using four laser pointers and a camera [12]. However, it estimates aircraft altitude under the assumption that the landing surface is flat. Additionally, this landing system has difficulty finding obstacles with laser pointers because the laser pointers are pointed straightly and so cannot find obstacles that are not directly in front. In contrast, ultrasonic sensors cover a wider area than laser pointers and can receive the reflected waves, so they are suitable for examining the safety of the landing area.

Therefore, we use ultrasonic sensors to determine whether the intended landing space is suitable. Their main advantages are that they are small, lightweight, and low cost. However, a conventional ultrasonic sensor can measure only the distance to the nearest object, and this information is insufficient to estimate the surface conditions of a landing space [13, 14].

Therefore, we propose a system that has the following four features.

- Short ultrasonic pulses

We have made it possible to detect both obstacles and the ground by making the pulse emitted from an ultrasound sensor extremely short. There is a method for recognizing multiple objects with one ultrasonic pulse, but a high-voltage pulse of 720 V must be generated so that the reflected wave increases quickly [15]. Such high voltages are difficult for drones to generate. Although there is a method that enables multiple objects to be recognized by using a single sine wave of 5 V, fast Fourier transform needs to be carried out on the host computer, and processing on a small drone is difficult [16].

Masatoshi Hamanaka is with RIKEN, Center for Advanced Intelligence Project, Japan (e-mail: masatoshi.hamanaka@riken.jp).

Fujio Nakano is with Kyoto University Unit of Synergetic Studies for Space, Japan (e-mail: naknet1@me.com).

- Improvement in voltage increase through reflected-wave integration
In our system, ultrasonic transmission units emit two ultrasonic pulses of 5 V. Since the received reflected waves are very small, they are amplified and integrated by using an operational amplifier so that a peak appears. Thus, the object can be visually recognized from this peak.
- Ultrasonic receiving unit for each arm
By installing an ultrasonic receiving unit on each arm of the drone and observing differences in the peaks of the acquired reflected waves, the flatness of the landing point can be determined.
- Suitability identification by deep learning
By using deep learning, it is possible to automatically identify whether a space is suitable for drone landing [17, 18]. The significance of using deep learning for determining suitability for landing is twofold: robust identification and reduced size and weight. For the former, suitable landing spaces can be robustly identified by accumulating data on successful and unsuccessful landings. For the latter, by carrying out deep learning on a single-chip field-programmable gate array, even a small lightweight drone can evaluate the landing space through autonomous flight [19].

We conducted experiments to evaluate our system and found that the reflected waves were small and changed irregularly for each sensor in spaces unsuitable for landing. Using deep learning, we could determine whether a space is suitable for drone landing with 98% accuracy. We explain how our system evaluates the surface conditions of the landing space using ultrasonic sensors in Section II and describe the implementations of the hardware and software in Sections III and IV, respectively. In Section V, we present and discuss the experimental results. In Section VI, we investigate the application of deep learning to the proposed system. We conclude with a brief summary and mention future plans in Section VII.

II. EVALUATING SURFACE CONDITIONS OF LANDING SPACE USING ULTRASONIC WAVES

A drone with our system can autonomously evaluate the suitability of a landing space before landing. A drone requires automatic landing when communication between the base station and the drone is interrupted or when a landing signal is transmitted from the base station to the drone.

First, the drone slowly descends while sensing with the ultrasonic sensors mounted underneath it. Since the measuring distance of the ultrasonic sensors is up to 5 m, when the distance from the ground surface or an obstacle becomes less than 5 m, the our system starts to evaluate surface conditions. If the landing space is determined to be suitable, the drone will continue sensing and descending and then land. If the landing space is not suitable, it will try landing somewhere else when returning to the take-off position.

The drone is always moving while hovering; therefore, if its position and altitude are accurately known, a point cloud of the landing space can in principle be created by mapping the distance indicated by the ultrasonic sensors in a three-dimensional (3D) space (Fig. 2).

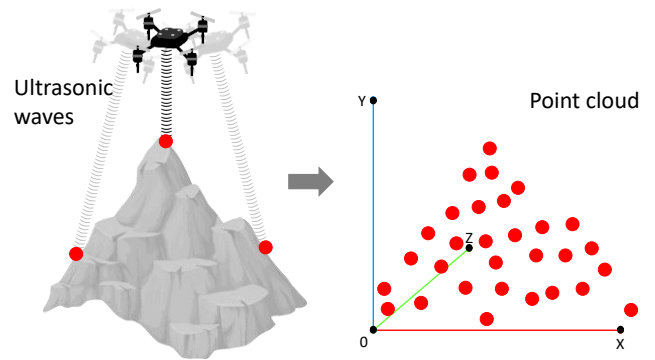


Figure 2. Point cloud from ultrasonic sensors on drone

A. Lack of GPS Accuracy

Since global positioning system (GPS) has an error of about 2 m, 3D shapes cannot be superimposed when creating a point cloud. By using real-time kinematic (RTK)-GPS [20], the accuracy will be within several centimeters and a point cloud can be created, but RTK-GPS is difficult to mount on a small lightweight drone.

Therefore, we do not create a point cloud but determine whether the surface conditions are suitable for landing. For conditions in which landing is not possible, it is not worth creating a precise point cloud.

B. Directivity of Ultrasonic Sensor

Ultrasonic waves are emitted in a beam form with a certain spread from the transducer. The spread is about 20 to 30 degrees; therefore, an ultrasonic sensor does not have pinpoint directivity, unlike radar. An ultrasonic sensor also has difficulty covering a wide area, unlike LiDAR.

Therefore, with our system, ultrasonic sensors are mounted on each arm of a drone, and reflected waves are compared to find obstacles during landing. If the distances indicated by each ultrasonic sensor are the same, the landing site is estimated to be flat. However, if are distances are indicated to be different, the landing space is estimated to contain an obstacle (Fig. 3).

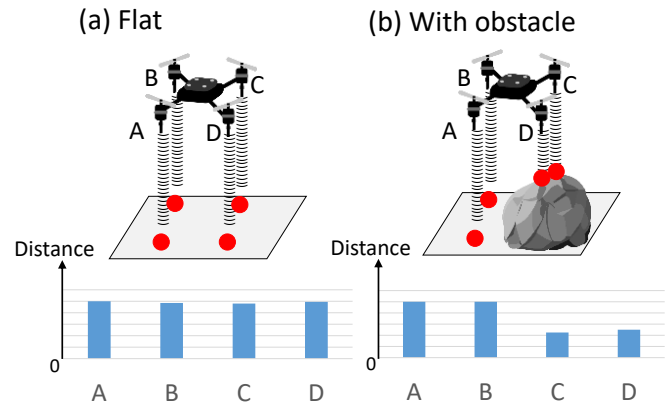


Figure 3. Obstacle detection with multiple ultrasonic sensors

C. Temporal Change

A conventional ultrasonic distance sensor captures the shortest reflected wave. For example, Distance A will be detected when using such a sensor on a stepped wall, as shown

in Fig. 4. Drones are constantly moving under the influence of the wind. In addition, vegetation and thin branches move with the wind generated by the drone. Therefore, in spaces containing vegetation or trees, the detection distance significantly changes due to wind. Therefore, the surface conditions of a landing space can be evaluated by distributing reflected waves.

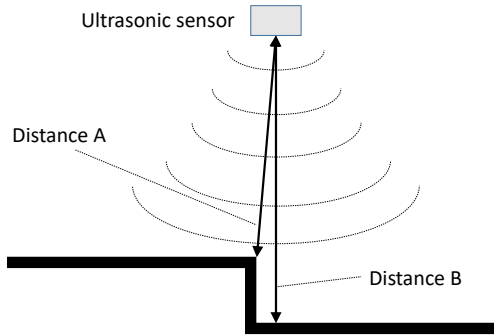


Figure 4. Detection distance of ultrasonic sensor on stepped wall

D. Distribution of Ultrasonic Reflected Waves

Figure 5 shows the difference between a system using conventional ultrasonic distance sensors and our system. A conventional ultrasonic distance sensor outputs a pulse of a certain length by using a transducer. The distance is then calculated by measuring the time until the reflected wave returns.

With our system, however, an ultrasonic sensor outputs only two pulses from the transducer. The pulses are then reflected back to various spaces and return. The reflection becomes an analog signal because the reflected waves are integrated. No special circuit is used for integration, the reflected waves overlap, and the signal strength increases.

If there is an obstacle on the ground, a conventional ultrasonic distance sensor can only determine the distance to the obstacle. However, with our system, there are two peaks: one corresponds to the distance to the obstacle, and the other corresponds to the distance to the ground. In fact, the distribution becomes more complicated than that in Fig. 5, and we can determine the surface conditions.

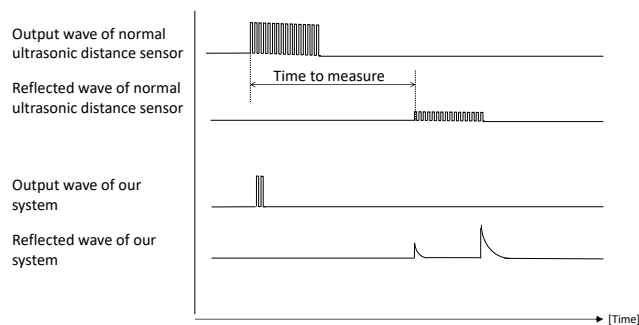


Figure 5. Comparison of system using conventional ultrasonic distance sensors and our system

III. HARDWARE IMPLEMENTATION

Figure 6 shows a prototype of our system for measuring surface conditions using ultrasonic waves. We constructed a quadcopter drone with an aluminum frame. Each transducer was mounted at the tip of the arm, and the receivers were mounted underneath the body.

Figure 7 shows the configuration of the system. First, every 50 ms, the central processing unit (CPU) outputs two pulses of 40 KHz at a transistor-transistor logic (TTL) level of 5 V. Then, the pulses are amplified by an amplifier and output from the ultrasonic transmission unit. As the two transmitted pulses are reflected from various objects, their signal strength changes over time. The time series of the signal strength obtained with the ultrasonic receiving units is amplified and integrated by the operational amplifiers, rectified by a diode, and then converted into an analog volume change. Analog volume changes are analog-to-digital converted by the CPU and stored in memory. The signal strength is stored at 1 byte per centimeter up to 5 m. Since 2000 bytes are required to store all four channels of reflective-waves, we use PICK18F26K22 as the CPU because it has sufficient memory. The four-channel distribution data are output via the RS-422 protocol and sent to a personal computer via a level conversion integrated circuit (IC) and serial-USB conversion IC.

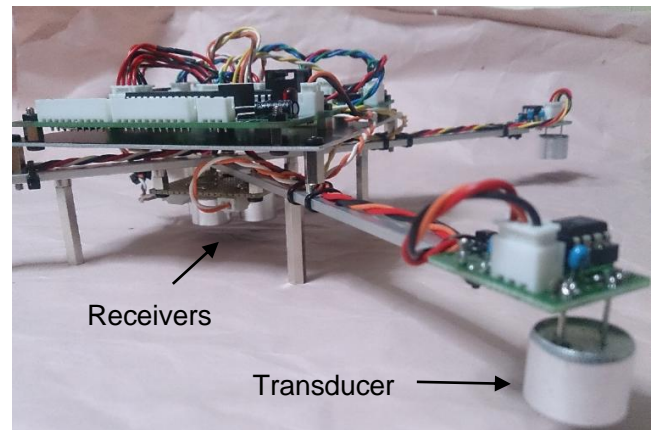


Figure 6. Prototype of proposed system

IV. SOFTWARE IMPLEMENTATION

We built Java software to display the distribution of reflected ultrasound signals, as shown in Fig 8. The horizontal axis of the graph is distance, from 0 to 500 cm. It is also possible to zoom in from 0 to 200 cm. The horizontal axis of the graph is the signal strength. The distribution graph is updated in real time. If the update is too fast, the visibility will be low, so the refresh rate can be selected from five options: 50, 100, 250, 500, and 1000 ms. A dip switch for switching the refresh rate is connected to the CPU on the hardware.

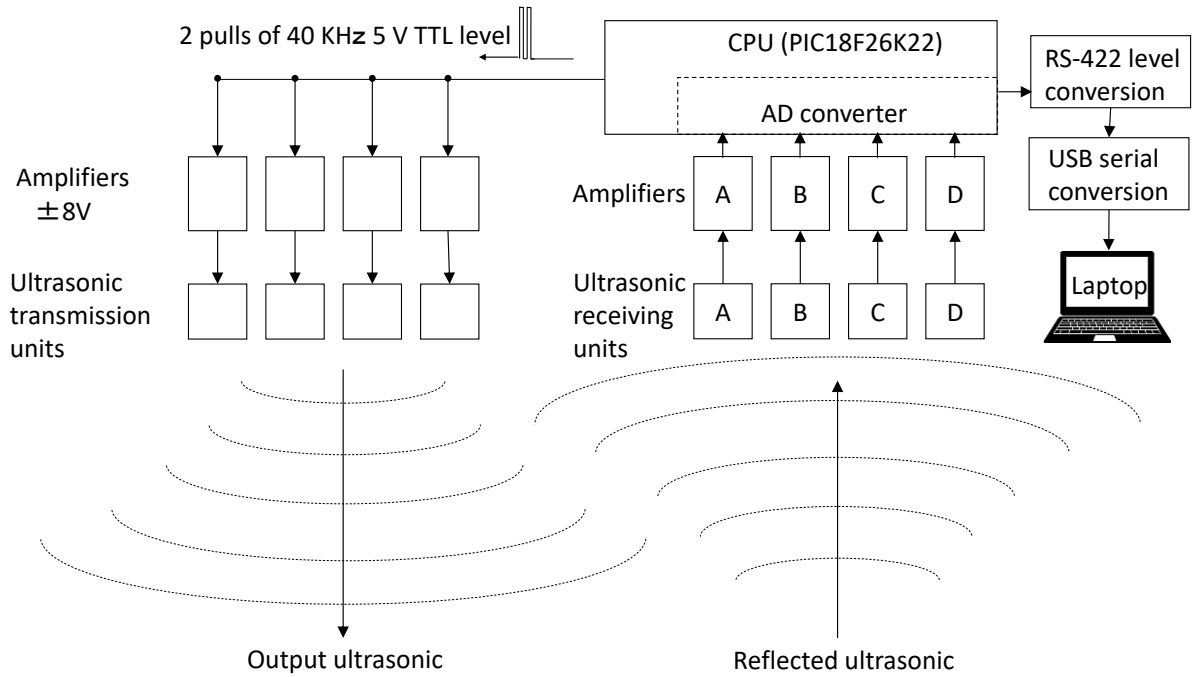


Figure 7. Configuration of proposed system

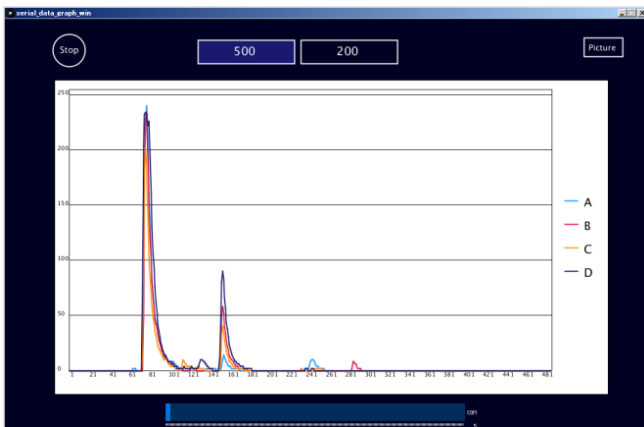


Figure 8. Display of distribution of reflected ultrasound signals with proposed system

V. EXPERIMENTAL RESULTS

We divided surface conditions of the landing space into three types (suitable for landing, not suitable for landing, and dangerous for landing) and measured the distribution of ultrasonic reflected signals at multiple points.

A. Suitable for Landing

The distribution of the reflected signals of the ultrasonic waves was measured on a wooden deck without a concrete slab. The drone hovered more than 1 m above the deck (Fig. 9). Figure 10 shows the reflected-signal distribution at that time, in which the peak was around 100 cm for all four channels, but the signal intensity significantly differed for each

channel. When a wooden board was placed on the deck, the signal strengths of all four channels were almost the same (Fig. 11). Ultrasonic waves went into the gaps in the wooden deck, causing a drop in reflectivity.



Figure 9. Wooden deck (left) and with board placed on top (right)

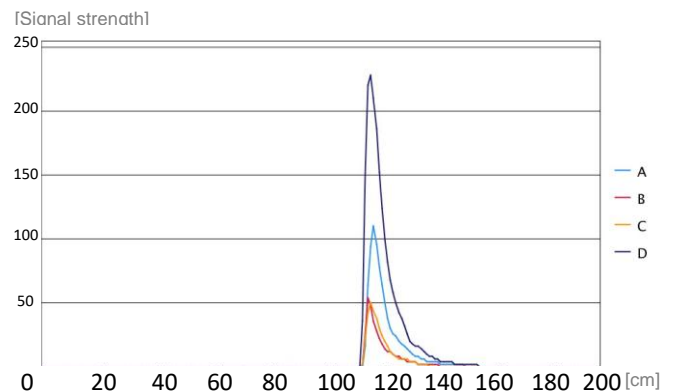


Figure 10. Reflected-signal distribution for wooden deck

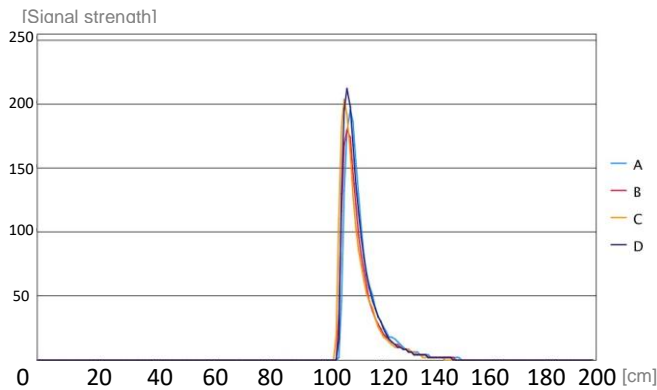


Figure 11. Results on wooden deck with wooden board

Hovering the drone 1 m above the concrete slab and placing a wooden board on the slab provided almost the same reflected-signal distribution as that in Fig. 11. When the wooden board was removed, the peak was near 1 m, as shown in Fig. 12, but there was a difference in the peak height. Because the concrete was rough due to aging, the ultrasonic waves were irregularly reflected, and the reflected waves were weakened. The measurement was also carried out when the drone hovered at 0.5 m (Fig. 13) and 1.7 m (Fig. 14). At 0.5 m, three-order reflected waves, i.e., waves reflected by the drone and those by the concrete slab, also appeared. At 1.7 m, the shape of the waveform resembled 1 m, but the signal strength was greatly attenuated. One characteristic of a space suitable for landing, such as a wooden deck or concrete slab, is that the reflection-intensity peaks of the four channels align.

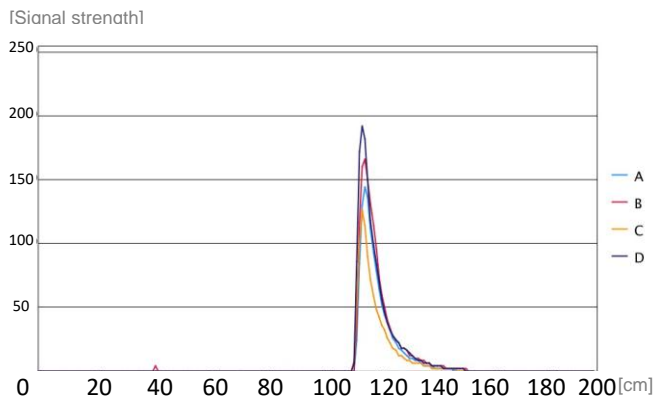


Figure 12. Reflected-signal distribution for concrete slab

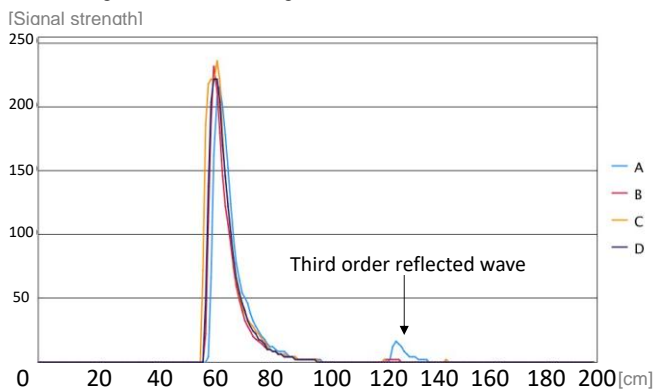


Figure 13. Reflected-signal distribution from 0.5 m above concrete slab

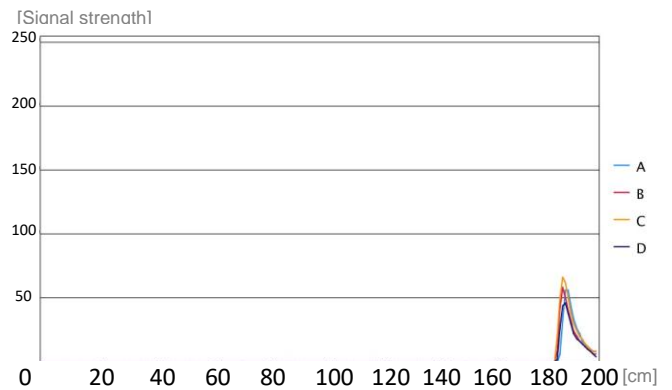


Figure 14. Reflected-signal distribution from 1.7 m above concrete slab

B. Not Suitable for Landing

We measured the reflected-signal distribution for an uneven space and spaces with sparse and thick vegetation, which are not suitable for landing. The uneven space was where animals (wild boars) had dug in search of food (Fig. 15) and presented a risk of the drone crashing during landing.

The space with sparse vegetation was covered with vegetation of about 35 cm in height, and the space with thick vegetation was on a 40-degree slope and covered with vegetation of about 50 cm in height (Fig. 15). The drone risks crashing when leaves become caught in its rotor.

Figures 16 and 17 show the results of the drone hovering 1 and 1.7 m above the uneven space, respectively. Since the ultrasonic waves were absorbed and diffused, the reflection intensity was very low but detectable.



Figure 15. Uneven space (left), space with sparse vegetation (center), and space with thick vegetation (left)

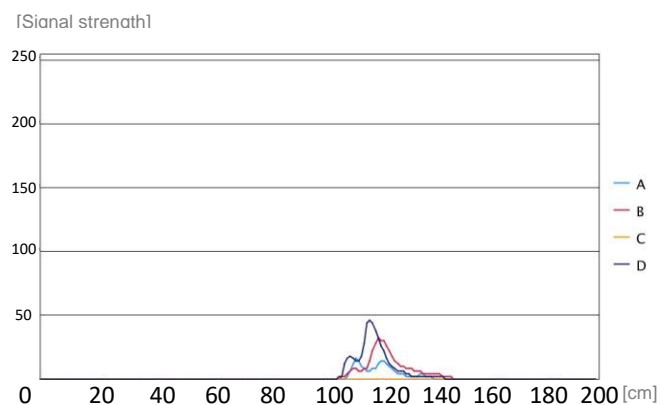


Figure 16. Reflected-signal distribution from 1.0 m above uneven space

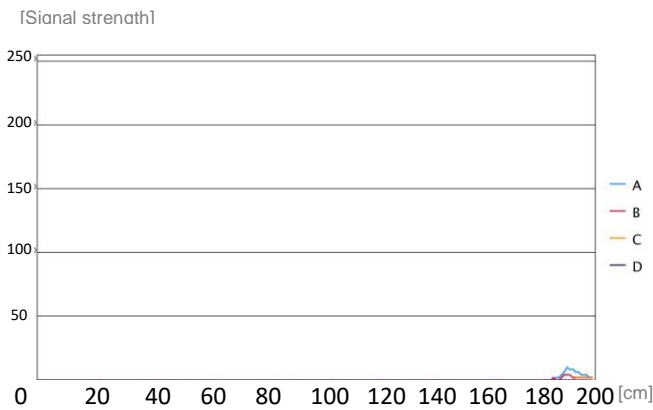


Figure 17. Reflected-signal distribution from 1.7 m above uneven space

Figure 18 shows the reflected-signal distribution when the drone hovered 1 m above the space with sparse vegetation. The reflection intensity varied depending on the leaf density and the direction of the leaf surface, but approximate flatness was determined.

Figure 19 shows the reflected-signal distribution when the drone hovered 1 m above the space with thick vegetation. Although the signal strength from the receivers toward the top of the slope had a sharp peak, the signal strength from the receivers toward the bottom had a gentle peak. A feature of surface conditions not suitable for landing, such as unevenness and vegetation, is that the reflection intensity of the four channels varies irregularly.

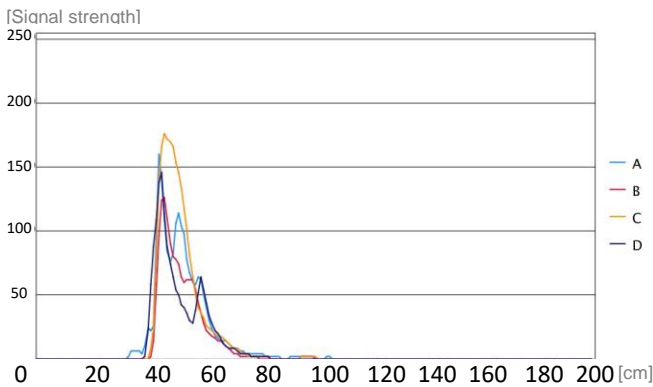


Figure 18. Reflected-signal distribution from 1.0 m above space with sparse vegetation

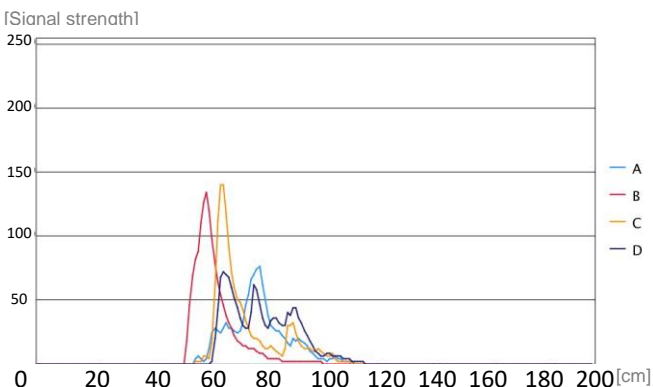


Figure 19. Reflected-signal distribution 1.0 m above space with thick vegetation

C. Dangerous for Landing

We measured the reflected-signal distribution where there was a stone and rock. In such spaces, the propellers, legs, or arms risk coming into contact with the stones and rocks, causing the drone to lose its balance and crash.

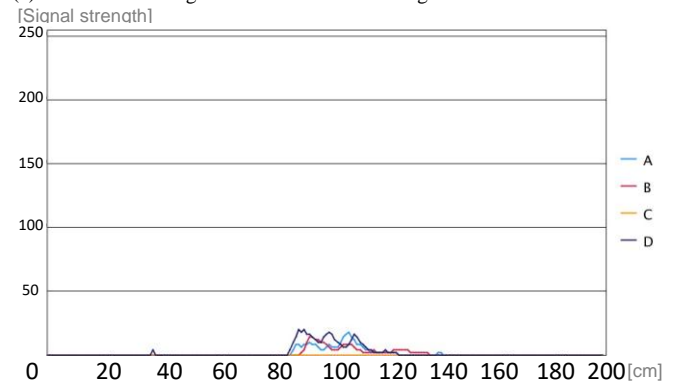
The stone was about 15 cm high, and the drone hovered 1 m above the ground. Figure 21 shows the reflected-signal distribution just above the stone. Although the space around the stone had sparse vegetation and was possible to land in, it was difficult to distinguish between the stone and vegetation due to the large amount of ultrasound diffusion and low reflection intensity (Fig. 21a). However, when viewed in chronological order, peaks were occasionally generated around 80 cm, so stones can possibly be identified by looking at the temporal change (Fig. 21b).

The rock was about 70 cm tall, and the drone hovered 1 m above the ground and thus 30 cm above the rock. Figure 22 shows the reflected-signal distribution, with a peak around 30 cm and the rock being recognized. There was also a peak near 1 m, and the ground was also recognized.



Figure 20. Stone (left) and rock (right)

(a) Difficult to distinguish between stone and vegetation



(b) Small peak at 60 cm

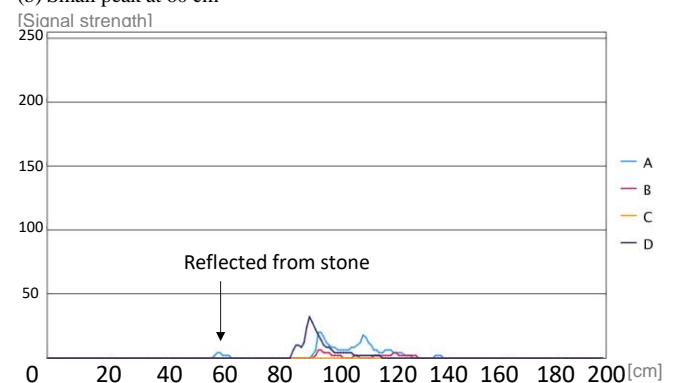


Figure 21. Reflected-signal distribution for stone and drone hovering at 1.0 m

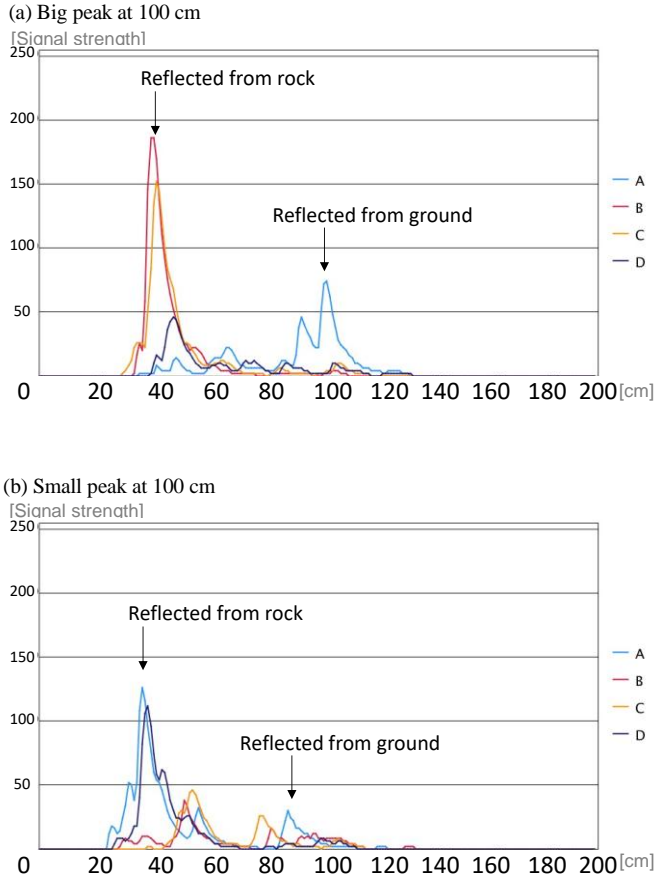


Figure 22. Reflected-signal distribution for rock and drone hovering at 1.0 m

VI. PROPOSED SYSTEM USING DEEP LEARNING

A simulation experiment was conducted to determine whether a space's suitability for landing can be estimated by using deep learning.

A. Determining Surface Conditions for Landing

When the following surface conditions are satisfied, a space is determined to be suitable for landing.

- Flatness of landing space
Except in a space where there are many irregular reflections of ultrasonic waves, such as uneven land, a maximum peak occurs at the position of the ground. If the four maximum peaks are almost at the same position (within 3 cm), the landing space is determined to be flat.
- No obstacles
Obstacles such as stones and rocks are difficult to recognize, as shown in Figs. 20 and 21. Therefore, any reflection at a distance shorter than the four maximum peaks is regarded as an obstacle.

B. Data Augmentation

The data acquired thus far using the drone are limited. Also, carrying out many measurements is costly. Therefore, the learning data is augmented by using the following data.

- Creating basic reflected waves
All collected reflected waves, as mentioned in Section V, are divided into basic reflected waves. A basic reflected wave is obtained by deleting a portion where the value of the original reflected wave is 0 and dividing the distribution into several distributions. Fifty basic reflected waves were extracted.
- Superposition of the basic reflected waves
Reflected waves are artificially generated by shifting the positions of the basic reflected waves and superimposing them. An artificial reflected wave has a vertical axis from 0 to 255 cm and a horizontal axis from 0 to 500 cm. The number of superimposed basic reflected waves is randomly determined between one and five. The shift in the distance direction is randomly determined between -250 and +250 cm, but excludes the cases in which a part of the fundamental reflected wave is 0 or less or the entire fundamental reflected wave exceeds 500 cm. The size of the fundamental reflected wave varies randomly in 0.1 steps from 0.1 to 3 times. If the vertical axis exceeds 255 as a result of the superposition, it is excluded.
- Determine the generated reflected wave
By using the method described in VI A, the generated reflected waves are determined as suitable or not for landing and labeled. We generated one million reflected waves suitable for landing and one million reflected waves not suitable for landing.

C. Learning and Evaluating by Deep Learning

We used a multi-layer perceptron (MLP) for learning the relationship between the generated reflected waves and the label. The input layer was a 2000-dimensional layer, i.e., 500-dimensional reflected wave from each of the four sensors. There were four intermediate layers, each having 1,000 units of perceptron (Fig. 23). We used 90% of the data as learning data and 10% as evaluation data. The accuracy of the data was 0.98; most of the incorrect data were when the maximum peaks of the four distributions were slightly longer than 3 cm.

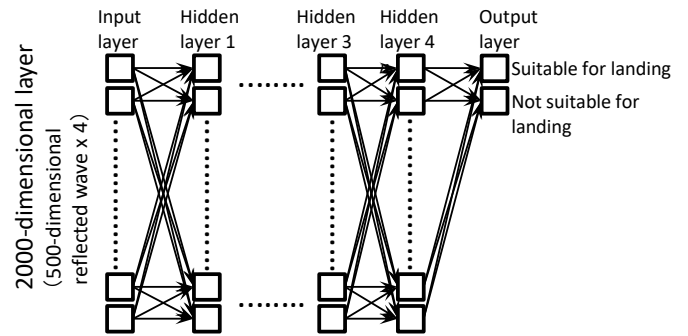


Figure 23. MLP for estimating surface conditions of landing space

VII. CONCLUSION

We proposed a system to evaluate the surface conditions of a space for a drone to land using ultrasonic sensors attached to each arm of the drone. The ultrasonic transmitting unit outputs two pulses of ultrasonic waves, and the receiving unit

receives the reflected waves. By integrating the received waves by using an operational amplifier and rectifying them by using a diode, a circuit is created that causes a peak at an object or on the ground.

The results indicate that, in spaces suitable for landing, the four peaks were all in the same place and that the surface flatness could be evaluated. In spaces not suitable for landing, the signals from the four sensors had irregular movements. In spaces dangerous for landing, there was another peak besides the ground. From results of a simulation experiment, our system could determine whether a space was suitable for landing with an accuracy of 0.98 by using deep learning.

We plan to construct an emergency landing system for a small lightweight drone [to use for detailed evaluations outdoors.

ACKNOWLEDGMENTS

This work was supported by the Japan Society for the Promotion of Science (JSPS KAKENHI Grant Number 17K19972).

REFERENCES

- [1] J. S. Wynn and T. W. McLain, "Visual Servoing for Multirotor Precision Landing in Daylight and After-Dark Conditions," 2019 International Conference on Unmanned Aircraft Systems (ICUAS2019), pp. 1242–1248, June 2019.
- [2] S. Lee, T. Shim, S. Kim, J. Park, K. Hong, and H. Bang, "Vision-Based Autonomous Landing of a Multi-Copter Unmanned Aerial Vehicle using Reinforcement Learning," 2018 International Conference on Unmanned Aircraft Systems (ICUAS2018), pp. 108–114, June 2018.
- [3] M. B. Vankadari, K. Das, C. M. Shinde, and S. Kumar, "A Reinforcement Learning Approach for Autonomous Control and Landing of a Quadrotor," 2018 International Conference on Unmanned Aircraft Systems (ICUAS2018), pp. 676–683, June 2018.
- [4] L. Nieto-Hernandez, A. A. Gomez-Casasola, and H. Rodriguez-Cortes, "Monocular SLAM Position Scale Estimation for Quadrotor Autonomous Navigation," 2019 International Conference on Unmanned Aircraft Systems (ICUAS2019), pp. 1359–1364, June 2019.
- [5] J. A. Lewis and E. N. Johnson, "Approximating UAV and Vision Feature Point Correlations in a Simplified SLAM problem," 2019 International Conference on Unmanned Aircraft Systems (ICUAS2019), pp. 1381–1388, June 2019.
- [6] S. V. Rothmund and T. A. Johansen, "Risk-Based Obstacle Avoidance in Unknown Environments using Scenario-Based Predictive Control for an Inspection Drone Equipped with Range Finding Sensors," 2019 International Conference on Unmanned Aircraft Systems (ICUAS2019), pp. 212–221, June 2019.
- [7] J. L. Sanchez-Lopez, C. Sampedro, D. Cazzato, and H. Voos, "Deep learning based semantic situation awareness system for multirotor aerial robots using LIDAR," 2019 International Conference on Unmanned Aircraft Systems (ICUAS2019), pp. 891–900, June 2019.
- [8] R. Opromolla, G. Fasano, G. Rufino, M. Grassi, and A. Savvaris, "LIDAR-inertial integration for UAV localization and mapping in complex environments," 2016 International Conference on Unmanned Aircraft Systems (ICUAS2016), pp. 649–656, June 2019.
- [9] D. Ma, A. Tran, N. Ket, R. Yanagi, P. Knight, K. Joglekar, N. Tudor, B. Cresta, and S. Bhandari, "Flight Test Validation of Collision Avoidance System for a Multicopter using Stereoscopic Vision," 2019 International Conference on Unmanned Aircraft Systems (ICUAS2019), pp. 981–987, June 2019.
- [10] E. Perez, A. Winger, A. Tran, C. Garcia-Paredes, N. Run, N. Ket, S. Bhandari, and A. Raheja, "Autonomous Collision Avoidance System for a Multicopter using Stereoscopic Vision," 2018 International Conference on Unmanned Aircraft Systems (ICUAS2018), pp. 579–588, June 2018.
- [11] M. Hamanaka, "Deep Learning based Area Estimation for Unmanned Aircraft Systems using 3D Map," 2018 International Conference on Unmanned Aircraft Systems (ICUAS2018), pp. 416–423, June 2018.
- [12] M. P. Degrande, E. E. T. Moreira, and E.M. Belo, "An Application of Digital Image Processing for UAV's Automatic Landing System Aid," 2014 International Council of the Aeronautical Sciences, ICAS2014_0915, 8 pages, 2014.
- [13] A. Carullo, and M. Parvis, "An Ultrasonic Sensor for Distance Measurement in Automotive Applications," IEEE Sensors Journal, Vol. 1, No. 2, August 2001.
- [14] V. A. Zhmud, N. O. Kondratiev, K. A. Kuznetsov, V. G. Trubin, and L. Dimitrov, "Application of ultrasonic sensor for measuring distances in robotics," Journal of Physics Conference Series 1015(3):032189, May 2018.
- [15] A. Ohya, T. Ohno, and S. Yuta, "Obstacle detectability of ultrasonic ranging system and sonar map understanding," Robotics and Autonomous Systems, 18(1-2), pp. 251–257, 1996.
- [16] M. Okugumo, "Development Research on Ultrasound Sensor System aiming at External Recognition of a Car," Research reports of Yonago National College of Technology, No. 48, pp. 22–26, March 2012.
- [17] Y. LeCun, Y. Bengio, and G. E. Hinton, "Deep Learning," Nature, Vol. 521, Issue 7553, pp. 436–444, 2015.
- [18] Amari S, Ozeki T, Karakida R, Yoshida Y, and Okada M, "Dynamics of Learning in MLP: Natural Gradient and Singularity Revisited," Neural Computer, Vol. 30, Issue 1, pp. 1–33, 2018.
- [19] A. Shawahna, S. M. Sait, and A. El-Maleh, "FPGA-Based Accelerators of Deep Learning Networks for Learning and Classification: A Review," IEEE Access, Vol. 7, pp. 7823–7859, December 2018.
- [20] M. Saito, Y. Ohmura, and A. Onoda "Network-based RTK-GPS for Nationwide High-accuracy Positioning and Navigation in Japan," Satellite Navigation Systems: Policy, Commercial and Technical Interaction, 151-158, 203.